9 Appendix 3: Geometry of TFC

9.1 Derivation of stiffness formulae

Below, the discrete models of the three different geometries have been translated into continuous models with a bending stiffness (EI) and a racking shear stiffness (GA). With these two characteristics, the stiffness of the discrete model can be approximated which enables;

- An optimisation of the efficiency via a more ideal distribution of the construction material over the different members
- A better understanding of the functioning of the construction
- An easy change of parameters (geometry, material) and assessment of the effect on the deflection

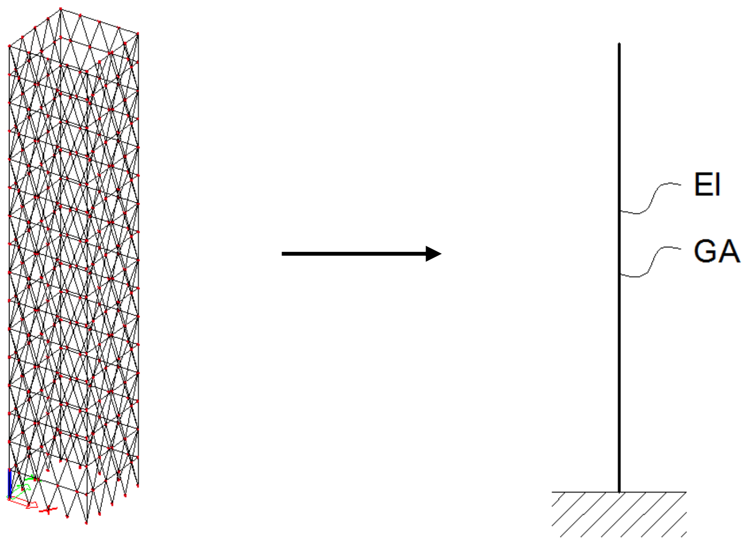

Figure 9.1: Discrete model versus continuous model

These formulae are derived for all three geometries hereafter referred to as;

- "vertical columns"
- "diagonal columns"
- "diagonal & vertical columns"

TFC variant: "Vertical columns"

The racking shear stiffness and the bending stiffness are first determined for the 2-dimensional trussed frame and then for the 3-dimensional trussed tube structure, as illustrated in Figure 9.2 and Figure 9.3, respectively.

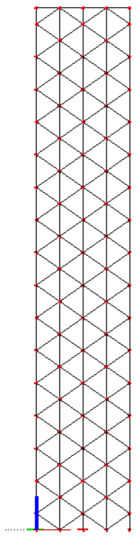

Figure 9.2: 2-dimensional variant "vertical columns"

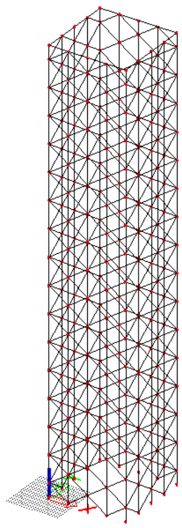

Figure 9.3: 3-dimensional variant "vertical columns"

Racking shear stiffness

The force F is spread evenly over the 4 diagonals in one horizontal section of the TFC. Due to force F the members undergo a shortening or a lengthening as illustrated in Figure 9.4.

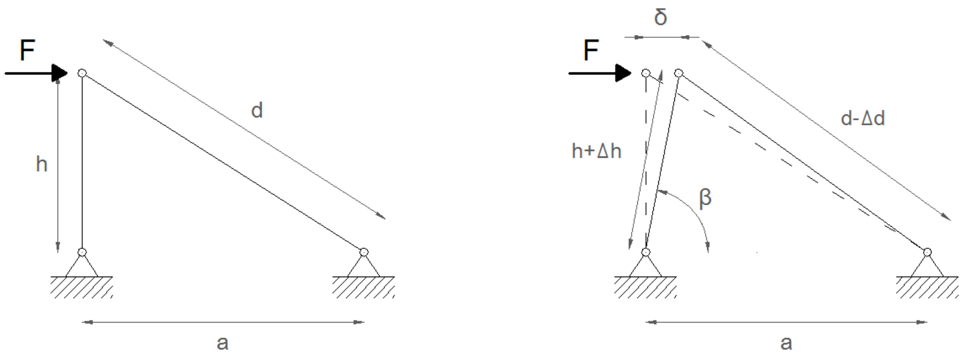

Figure 9.4: Section of a quarter-side of the variant "vertical columns"

With the help of the cosinus-rule, the horizontal deflection (δ) due to a force (F) can be calculated:

$$\cos(\beta)\,2ah = a^2 + h^2 - d^2$$

$$\frac{\delta}{(h+\Delta h)}2a(h+\Delta h) = a^2 + (h+\Delta h)^2 - (d-\Delta d)^2$$

$$2\delta a = a^2 + h^2 + 2h\Delta h + \Delta h^2 - d^2 + 2d\Delta d - \Delta d^2$$

Given that $a^2 + h^2 - d^2 = 0$ (Pythagoras' theorem), and that $\Delta d^2 \ll \Delta d$, the equation can be simplified:

$$2\delta a = 2h\Delta h + 2d\Delta d$$

$$\delta_{discrete} = \frac{h\Delta h}{a} + \frac{d\Delta d}{a}$$

This is the discrete function for the horizontal deflection (δ) as the sum of the bending deflection (lengthening of the vertical) and the shear deflection (shortening of the diagonal), respectively. The continuous function for horizontal deflection, with one concentrated load at the top is given by:

$$\delta_{continuous} = \frac{Fh^3}{3EI} + \frac{Fh}{GA}$$

Analogous, the continuous function for the horizontal deflection (δ) is the sum of the bending deflection and the shear deflection. Subsequently, the parameter for shear deflection from the discrete function can be equated with the parameter from the continuous function:

$$\frac{d\Delta d}{a} = \frac{Fh}{GA}$$

$$GA = \frac{Fha}{d\Delta d}$$

With:

$$\Delta d = F\frac{d}{a}\frac{d}{EA_d}$$

The formula can be written as:

$$GA = \frac{a^2hEA_d}{d^3}$$

However, this formula only gives the racking shear stiffness for one diagonal, whereas the 2-dimensional variant has 4 diagonals. Therefore, the racking shear stiffness needs to be multiplied by four, to give the correct formula for the trussed façade frame:

$$GA = \frac{4a^2hEA_d}{d^3}$$

In the case of the trussed tube structure, the expression for the racking shear stiffness needs to be multiplied by two since shear occurs in the two web planes of the tube. The formula for the tube structure is:

$$GA = 2 \cdot \frac{4a^2hEA_d}{d^3}$$

<u>Bending stiffness</u>

The gross bending stiffness can be determined with:

$$EI_y = \mathrm{E}I_{own;y} + \mathrm{E}A_v y^2$$

Here, $\mathrm{EI_{own;y}}$ does not contribute to the bending stiffness since the connections are modeled as pinned nodes. The other parameter $\Sigma\mathrm{E}A_v y^2$ represents the bending stiffness from the axial stiffness of the vertical members. Therefore the formula for the bending stiffness becomes:

$$EI_y = \mathrm{E}A_v y^2$$

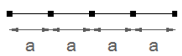

Figure 9.5: Plan of 2-dimensional geometry "vertical columns"

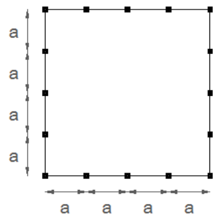

Figure 9.6: Plan of 3-dimensional geometry "vertical columns"

In the case of the 2-dimensional construction, with 5 columns, the formula is:

$$EI_y = \mathrm{E}A_v(2 \cdot a^2 + 2 \cdot 2a^2) = 10a^2 EA_v$$

In the case of the 3-dimensional construction, with 16 columns arranged in an orthogonal grid, the formula can be written as:

$$EI_y = \mathrm{E}A_v(4 \cdot a^2 + 10 \cdot 2a^2) = 44a^2 EA_v$$

The term 'E' in the abovementioned 2 formulae represent the Young's modulus of the construction material.

TFC variant: “diagonal columns”

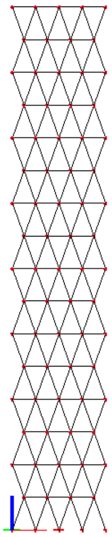

Figure 9.7: 2-dimensional variant “diagonal columns”

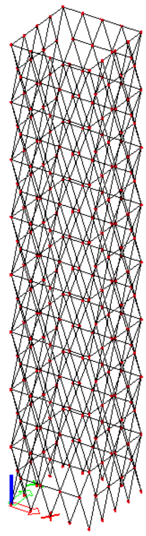

Figure 9.8: 3-dimensional variant “diagonal columns”

Racking shear stiffness

To determine the racking shear stiffness, a force F is spread over the diagonals in one horizontal section of the TFC. The assumption is made that the force is spread more or less evenly over the 4 diagonal.

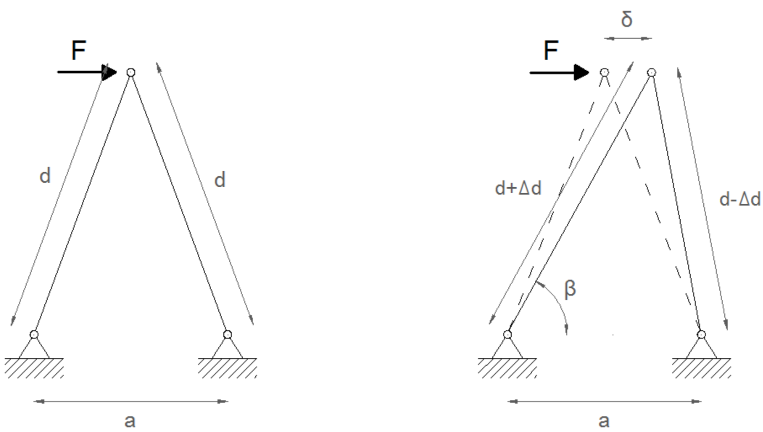

Figure 9.9: Section of a quarter-side of the variant “diagonal columns”

Due to force F the diagonal members undergo a shortening or a lengthening. With the help of the cosinus-rule, the horizontal deflection (δ) can be calculated:

$$\cos(\beta)\,2ac = a^2 + c^2 - b^2$$

$$\frac{\delta + 1/2a}{(d + \Delta d)}2a(d + \Delta d) = a^2 + (d + \Delta d)^2 - (d - \Delta d)^2$$

$$\left(\delta + \frac{1}{2}a\right)2a = a^2 + d^2 + 2d\Delta d + \Delta d^2 - d^2 + 2d\Delta d - \Delta d^2$$

$$\left(\delta + \frac{1}{2}a\right)2a = a^2 + 4d\Delta d$$

$$\left(\delta + \frac{1}{2}a\right) = \frac{1}{2}a + \frac{2d\Delta d}{a}$$

$$\delta_{discrete} = \frac{2d\Delta d}{a}$$

Note that this discrete function only holds an equation for shear deflection since bending deflection does not occur in the section considered here. By equating the discrete with the continuous function for horizontal deflection – with one concentrated load at the top – the racking shear stiffness can be determined:

$$\delta_{continuous} = \frac{Fh}{GA}$$

$$\frac{2d\Delta d}{a} = \frac{Fh}{GA}$$

$$GA = \frac{Fha}{2d\Delta d}$$

With:

$$\Delta d = F\frac{d}{a}\frac{2d}{EA_d}$$

The formula becomes:

$$GA = \frac{a^2 hEA_d}{2d^3}$$

Since four triangles are present per horizontal section the racking shear stiffness needs to be multiplied by four to find the total racking shear stiffness:

$$GA = \frac{2a^2 hEA_d}{d^3}$$

In the case of the trussed tube structure, the expression for the racking shear stiffness needs to be multiplied with two since shear occurs in the two web planes of the tube. The formula for the tube structure is:

$$GA = 2 \cdot \frac{2a^2 hEA_d}{d^3}$$

Bending stiffness

The bending stiffness comprises Young's modulus, dependent on the construction material, and the moment of inertia, which can be calculated with Steiner's theorem:

$$I_y = \Sigma A_{equ} y^2$$

However an equivalent section (A_{equ}) needs to be derived for the moment of inertia. This equivalent section is found by deriving equivalent formulae for the shortening of the diagonals and lengthening of the horizontal, and then combining them. The deformation of such a rhomboid can be seen in Figure 9.10.

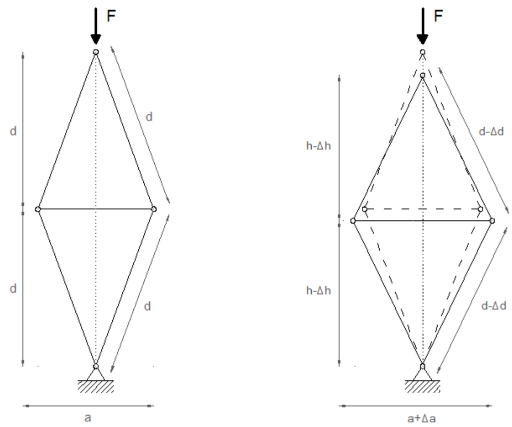

Figure 9.10: Deformation of an 'equivalent section'

<u>Shortening of the diagonals</u>

Figure 9.11 represents the schematization of the shortening of the diagonal.

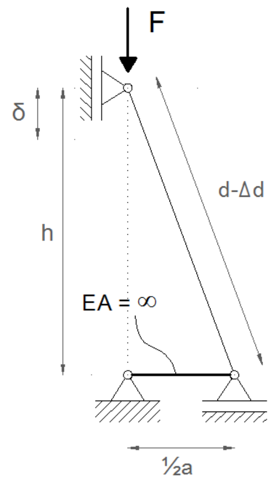

Figure 9.11: Part of the equivalent section: shortening of the diagonal

The force in the diagonal can be expressed as:

$$F_d = F \cdot \frac{d}{h}$$

And the shortening of the diagonal member can subsequently be written as:

$$\Delta d = F\frac{d}{h}\cdot\frac{d}{EA_d} = \frac{Fd^2}{hEA_d}$$

Pythagoras' theorem gives:

$$(h-\delta)^2 = (d-\Delta d)^2 - (\tfrac{1}{2}a)^2$$

$$h^2 - 2h\delta + \delta^2 = d^2 - 2d\Delta d + \Delta d^2 - (\tfrac{1}{2}a)^2$$

Given that $(\frac{1}{2}a)^2 + h^2 - d^2 = 0$ (Pythagoras' theorem), that $\Delta d^2 \ll \Delta d$, and that $\delta^2 \ll \delta$ the equation can be simplified:

$$2h\delta = 2d\Delta d$$

$$\delta = \frac{d\Delta d}{h}$$

After substitution of Δd the formula becomes:

$$\delta = \frac{d}{h}\cdot\frac{Fd^2}{hEA_d} = \frac{Fd^3}{h^2EA_d}$$

The displacement δ can be equated with the formula for the shortening of a member due to a normal force. However the abovementioned formula only takes one diagonal into account; since there are 2 per rhomboid (equivalent section), the formula needs to be multiplied by 2 as well :

$$\delta = \frac{Fd^3}{2h^2EA_d} = \frac{Fh}{EA_{equ;1}}$$

$$\frac{d^3}{2h^2A_d} = \frac{h}{A_{equ;1}}$$

$$A_{equ;1} = \frac{2h^3}{d^3}\cdot A_d$$

<u>Lengthening of the horizontal</u>
Figure 9.12 represents the schematization of the lengthening of the horizontal.

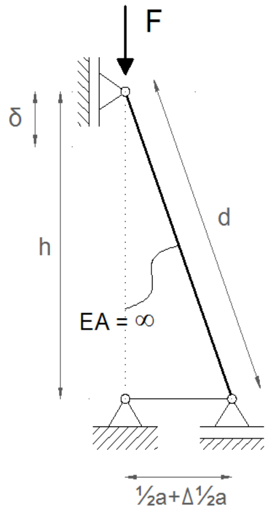

Figure 9.12: Part of the equivalent section: lengthening of the horizontal

The force in the horizontal can be expressed as:

$$F_a = F \cdot \frac{\frac{1}{2}a}{h}$$

And the lengthening of the horizontal member can subsequently be written as:

$$\Delta\tfrac{1}{2}a = F\frac{\frac{1}{2}a}{h} \cdot \frac{\frac{1}{2}a}{EA_h} = \frac{F(\frac{1}{2}a)^2}{hEA_h}$$

Pythagoras' theorem gives:

$$(h-\delta)^2 + (\tfrac{1}{2}a + \Delta\tfrac{1}{2}a)^2 = (d)^2$$

$$h^2 - 2h\delta + \delta^2 = d^2 - (\tfrac{1}{2}a)^2 - \tfrac{1}{2}a\Delta a - (\Delta\tfrac{1}{2}a)^2$$

Given that $(\frac{1}{2}a)^2 + h^2 - d^2 = 0$ (Pythagoras' theorem), that $(\Delta\frac{1}{2}a)^2 \ll \Delta\frac{1}{2}a$, and that $\delta^2 \ll \delta$ the equation can be simplified:

$$2h\delta = \tfrac{1}{2}a\Delta a$$

$$\delta = \frac{\frac{1}{4}a\Delta a}{h}$$

After substitution of Δd the formula becomes:

$$\delta = \frac{\frac{1}{2}a}{h} \cdot \frac{F(\frac{1}{2}a)^2}{hEA_h} = \frac{F(\frac{1}{2}a)^3}{h^2EA_h}$$

The displacement δ can be equated with the formula for the shortening of a member due to a normal force:

$$\delta = \frac{F(\frac{1}{2}a)^3}{h^2 EA_h} = \frac{Fh}{EA_{equ;2}}$$

$$\frac{(\frac{1}{2}a)^3}{h^2 A_h} = \frac{h}{A_{equ;2}}$$

$$A_{equ;2} = \frac{h^3}{(\frac{1}{2}a)^3} \cdot A_h$$

Now that $A_{equ;1}$ and $A_{equ;2}$ are known, both can be combined into one formula: A_{equ} the is the inverse sum of the formulae for $A_{equ;1}$ and $A_{equ;2}$:

$$\frac{1}{A_{equ}} = \frac{1}{A_{equ;1}} + \frac{1}{A_{equ;2}}$$

$$\frac{1}{A_{equ}} = \frac{d^3}{2 \cdot h^3 \cdot A_d} + \frac{(\frac{1}{2}a)^3}{h^3 \cdot A_h}$$

$$A_{equ} = \left(\frac{d^3}{2 \cdot h^3 \cdot A_d} + \frac{(\frac{1}{2}a)^3}{h^3 \cdot A_h}\right)^{-1}$$

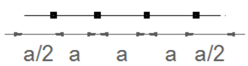

Figure 9.13: Plan of 2-dimensional geometry "diagonal columns"

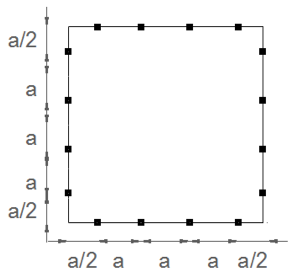

Figure 9.14: Plan of 3-dimensional geometry "diagonal columns"

Subsequently, the bending stiffness can be calculated by multiplying the moment of inertia by Young's modulus:

$$EI_y = \mathrm{E}A_{equ}(2 \cdot (\tfrac{1}{2}a)^2 + 2 \cdot (\tfrac{3}{2}a)^2) = 5a^2 EA_{equ}$$

In the case of the 3-dimensional construction, with 16 columns arranged in an orthogonal grid, the formula can be written as:

$$EI_y = \mathrm{E}A_{equ}(4 \cdot (\tfrac{1}{2}a)^2 + 4 \cdot (\tfrac{3}{2}a)^2 + 8 \cdot (2a)^2) = 42a^2 EA_{equ}$$

TFC variant: “diagonal & vertical columns”

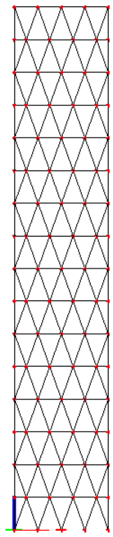

Figure 9.15: 2-dimensional variant “diagonal & vertical columns”

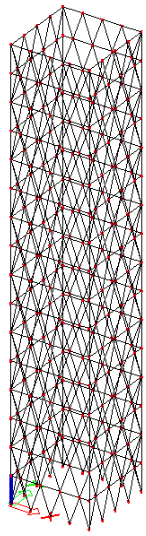

Figure 9.16: 3-dimensional variant “diagonal & vertical columns”

Racking shear stiffness

The racking shear stiffness (GA) of this variant is equal to the racking shear stiffness of the TFC variant “diagonal columns”: the vertical columns at the corners do not affect it. The formula for the trussed façade frame is:

$$GA = \frac{2a^2 hEA_d}{d^3}$$

And the formula for the trussed tube structure is:

$$GA = 2 \cdot \frac{2a^2 hEA_d}{d^3}$$

Bending stiffness

The bending stiffness comprises Young’s modulus, dependent on the construction material, and the moment of inertia, which can be calculated with Steiner’s theorem:

$$I_y = \Sigma A_{equ} y^2 + \Sigma A_d y^2$$

Where the equivalent section (A_{equ}) is the same as for the geometry variant “diagonal columns”:

$$A_{equ} = \left(\frac{d^3}{2 \cdot h^3 \cdot A_d} + \frac{(\frac{1}{2}a)^3}{h^3 \cdot A_h} \right)^{-1}$$

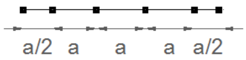

Figure 9.17: Plan of 2-dimensional geometry "diagonal & vertical columns"

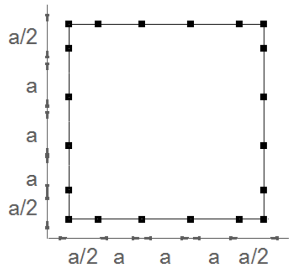

Figure 9.18: Plan of 3-dimensional geometry "diagonal & vertical columns"

In the case of the 2-dimensional construction, with 4 equivalent plus 2 vertical columns, the formula is:

$$EI_y = \mathrm{E}A_{equ}(2 \cdot (\tfrac{1}{2}a)^2 + 2 \cdot (\tfrac{3}{2}a)^2) + \mathrm{E}A_v(2 \cdot (2a)^2) = \mathrm{E}a^2(5A_{equ} + 8A_v)$$

In the case of the 3-dimensional construction, with 16 equivalent plus 4 vertical columns arranged in an orthogonal grid, the formula can be written as:

$$EI_y = \mathrm{E}A_{equ}(4 \cdot (\tfrac{1}{2}a)^2 + 4 \cdot (\tfrac{3}{2}a)^2 + 8 \cdot (2a)^2) + \mathrm{E}A_v(4 \cdot (2a)^2) = \mathrm{E}a^2(42A_{equ} + 16A_v)$$

Summary

The formulae for all three geometry variants are summarized in Table 9.1.

"vertical columns"	2-D	3-D
Racking shear stiffness	$GA = \frac{4a^2hEA_d}{d^3}$	$GA = 2 \cdot \frac{4a^2hEA_d}{d^3}$
Bending stiffness	$EI = 10a^2\mathrm{E}A_v$	$EI = 44a^2EA_v$
"diagonal columns"		
Racking shear stiffness	$GA = \frac{2a^2hEA_d}{d^3}$	$GA = 2 \cdot \frac{2a^2hEA_d}{d^3}$
Bending stiffness	$EI = 5a^2\mathrm{E}A_{equ}$	$EI = 42a^2EA_{equ}$
"diagonal & vertical columns"		
Racking shear stiffness	$GA = \frac{2a^2hEA_d}{d^3}$	$GA = 2 \cdot \frac{2a^2hEA_d}{d^3}$
Bending stiffness	$EI = Ea^2(5A_{equ} + 8A_v)$	$EI = Ea^2(42A_{equ} + 16A_v)$

Table 9.1: Overview of the stiffness formulae per geometry variant.

With

$$A_{equ} = \left(\frac{d^3}{2 \cdot h^3 \cdot A_d} + \frac{(\frac{1}{2}a)^3}{h^3 \cdot A_h}\right)^{-1}$$

9.2 Load – deformation formulae

To calculate the shear deflection and bending deflection by hand, formulae need to be derived as well. The starting points are that 16 concentrated loads are present with the same value and evenly distributed along the height.

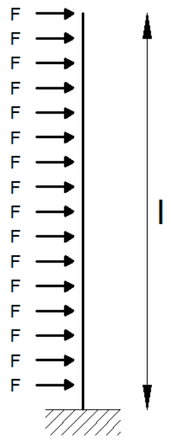

Figure 9.19: Load pattern on construction

<u>Bending deflection</u>
The bending deflection formula for a cantilevered rod with 16 concentrated loads can be derived with help of two existing formulae for a rod with one concentrated load at the top.

The deflection at the top:

$$y = \frac{Fl^3}{3EI}$$

The rotation at the top:

$$\varphi = \frac{Fl^2}{2EI}$$

These 2 formulae need to be combined several times to derive the formula for a rod with 16 concentrated loads based on a cumulative principle:

$$y_i = \Sigma(y_i + \varphi_i l_i)$$

$$y_{bending} = \frac{F}{EI}\Big(\frac{{}^{1}\!/_{16}\, l^3}{3} + \frac{{}^{1}\!/_{16}\, l^2}{2} \cdot \tfrac{15}{16} l + \frac{{}^{2}\!/_{16}\, l^3}{3} + \frac{{}^{2}\!/_{16}\, l^2}{2} \cdot \tfrac{14}{16} l + \frac{{}^{3}\!/_{16}\, l^3}{3} + \frac{{}^{3}\!/_{16}\, l^2}{2} \cdot \tfrac{13}{16} l$$

$$+ \;\dots\dots\dots + \frac{{}^{15}\!/_{16}\, l^3}{3} + \frac{{}^{15}\!/_{16}\, l^2}{2} \cdot \tfrac{1}{16}\Big)$$

$$y_{bending} = 2\frac{65}{384}\frac{Fl^3}{EI}$$

Shear deflection

The shear deflection formula for a cantilevered rod with 16 concentrated loads can be derived with help of the existing formula for a rod with one concentrated load at the top:

$$y = \frac{Fl}{GA}$$

$$y_i = \Sigma y_i$$

$$y_{shear} = \frac{1}{GA}\left({}^{1}/_{16}\, l \cdot F + {}^{1}/_{16}\, l \cdot 2F + {}^{1}/_{16}\, l \cdot 3F + \ \dots\dots\dots + {}^{1}/_{16}\, l \cdot 16F\right)$$

$$y_{shear} = 8\frac{1}{2}\frac{Fl}{GA}$$

NB: The bending deflection and shear deflection formulae for a cantilevered rod under a uniformly distributed load (q) could have been used as well, and can be found in the literature easily. However, the formulae from the literature would yield a different outcome and therefore different deviations, that are not present with the derived formulae for the deflection. Hence, the derived formulae guarantee a more accurate result.

9.3 Differences hand & ESA PT calculations

Now that the formulae for the EI and GA of the geometries are known, the hand results can be compared with the results of the discrete model computed by ESA PT. The deflection is split up into the bending deflection and the shear deflection to analyse the differences more exactly. All geometries are discussed at which the 2-dimensional construction and 3-dimensional construction are treated, respectively.
To increase the reliability of the comparison, the sections of the structural members have been varied. However, the maximum difference between the sections has been limited to a factor 4. In other words, the section of the largest member is 4 times larger than the section of the smallest member. The factor 4 is based on the fact that it is not likely that the sections will differ more, due to the connections that need to be in proportion. The two sections that have been adopted are;

CHS 457.0/40.0	$A = 5.24 \cdot 10^{-2}\ m^2$	O
CHS 273.0/16.0	$A = 1.29 \cdot 10^{-2}\ m^2$	o

Hand calculations
For a better understanding, one example calculation is given below for the 3-dimensional TFC variant "vertical columns"

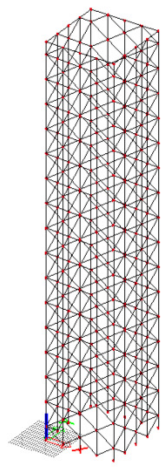

h =	5.25 m
a =	7.5 m
d =	9.15 m
F =	2000 kN
l =	168 m
E =	$2.1 \cdot 10^{8}$ kN/m^2
$A_{verticals}$ =	$5.24 \cdot 10^{-2}$ m^2
$A_{diagonals}$ =	$5.24 \cdot 10^{-2}$ m^2

$$EI = 44a^2EA_v = 44 \cdot 7.5^2 \cdot 2.1 \cdot 10^8 \cdot 5.24 \cdot 10^{-2} = 2.72 \cdot 10^{10}\ kNm^2$$

$$y_{EI} = 2\frac{65}{384}\frac{Fl^3}{EI} = 2\frac{65}{384} \cdot \frac{2000 \cdot 168^3}{2.72 \cdot 10^{10}} = 755 \cdot 10^{-3}\ m$$

$$GA = 2 \cdot \frac{4a^2hEA_d}{d^3} = 2 \cdot \frac{4 \cdot 7.5^2 \cdot 5.25 \cdot 2.1 \cdot 10^8 \cdot 5.24 \cdot 10^{-2}}{9.15^3} = 3.39 \cdot 10^7\ kN$$

$$y_{GA} = 8\frac{1}{2}\frac{Fl}{GA} = 8\frac{1}{2} \cdot \frac{2000 \cdot 168}{3.39 \cdot 10^7} = 84.3 \cdot 10^{-3}\ m$$

$$y_{total} = 755 \cdot 10^{-3} + 84.3 \cdot 10^{-3} = 840 \cdot 10^{-3}\ m = 840\ mm$$

ESA PT models
The ESA PT models have been built so they resemble the hand models as closely as possible: naturally, the geometries match those of the hand calculations exactly. And all connections are hinged, to eliminate bending and shear in the members.

To distinguish the shear deflection and bending deflection, two models have been built: one that is only supported at the base to compute the total deflection, as illustrated in Figure 9.20; and another identical one, where the nodes can only undergo a horizontal movement to compute the shear deflection, as illustrated in Figure 9.21. The bending deflection is obtained by subtracting the shear deflection from the total deflection.

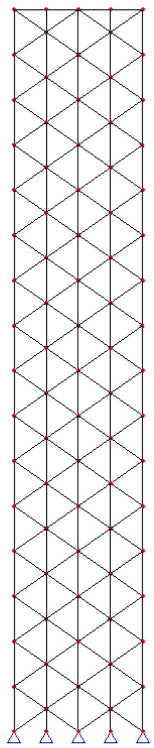

Figure 9.20: ESA model for total deflection

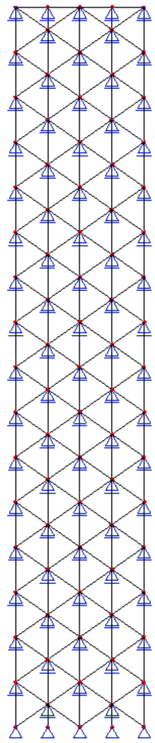

Figure 9.21: ESA model for shear deflection

TFC variant "vertical columns"

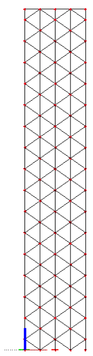

Figure 9.22: 2-dimensional variant

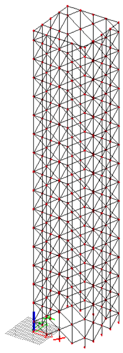

Figure 9.23: 3-dimensional variant

A (m^2)		δ	Hand (mm)	SCIA ESA PT (mm)	difference
A_v = 5.24e-2	O	$\delta_{bending}$	1662	1645	1.0%
A_d = 5.24e-2	O	δ_{shear}	84.30	84.4	-0.1%
		δ_{total}	1746	1729	1.0%
A_v = 1.29e-2	o	$\delta_{bending}$	6750	6683	1.0%
A_d = 1.29e-2	o	δ_{shear}	342.4	342.9	-0.1%
		δ_{total}	7093	7026	0.9%
A_v = 1.29e-2	o	$\delta_{bending}$	6750	6591	2.4%
A_d = 5.24e-2	O	δ_{shear}	84.30	84.5	-0.2%
		δ_{total}	6834	6676	2.3%
A_v = 5.24e-2	O	$\delta_{bending}$	1662	1661	0.0%
A_d = 1.29e-2	o	δ_{shear}	342.4	342.6	-0.1%
		δ_{total}	2004	2004	0.0%

Table 9.2: Differences 2-dimensional geometry variant "vertical columns".

A (m^2)		δ	Hand (mm)	SCIA ESA PT (mm)	difference
A_v = 5.24e-2	O	$\delta_{bending}$	755	748	1.0%
A_d = 5.24e-2	O	δ_{shear}	84.30	84.4	-0.1%
		δ_{total}	840	832.4	0.9%
A_v = 1.29e-2	o	$\delta_{bending}$	3068	3039	1.0%
A_d = 1.29e-2	o	δ_{shear}	342.4	342.9	-0.1%
		δ_{total}	3411	3381.9	0.8%
A_v = 1.29e-2	o	$\delta_{bending}$	3068	2930	4.5%
A_d = 5.24e-2	O	δ_{shear}	84.30	84.5	-0.2%
		δ_{total}	3153	3014.5	4.4%
A_v = 5.24e-2	O	$\delta_{bending}$	755	794	-5.1%
A_d = 1.29e-2	o	δ_{shear}	342.4	342.6	-0.1%
		δ_{total}	1098	1136.6	-3.5%

Table 9.3: Differences 3-dimensional geometry variant “vertical columns”.

TFC variant “vertical columns”

Regarding the 2-dimensional variant; in case 1 and 2 where the verticals and diagonals have equal sections, the deflection only differs marginally where the computer calculation yields a higher value. Yet, this difference can be understood from the results from the 3rd and 4th comparison where the influence of the diagonals is becomes clear: In case the diagonals have a large section and the verticals a small section, the hand calculation gives a greater deflection which can be primarily attributed to the bending deflection. In other words, the bending stiffness calculated via the mechanics formula is smaller. This result can be ascribed to the influence of the diagonals that has been discarded for the bending stiffness: when the verticals shorten, the diagonals have to shorten as well and will provide a certain resistance, depending on their tensile rigidity, as illustrated in Figure 9.24.

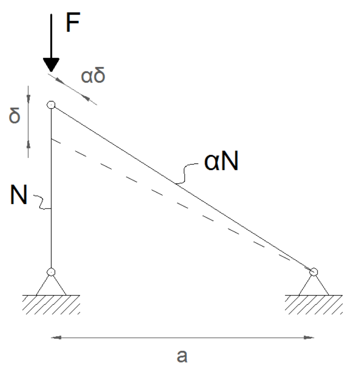

Figure 9.24: Contribution of the diagonal due to its shortening

This means that if the diagonals have relatively large sections compared to the verticals, the tensile rigidity and thus the bending stiffness of the 2-dimensional construction increases. In case the diagonals have a small section and the verticals a large section, the hand and computer calculation give nearly the same answer. This

can be explained by the inversing the abovementioned phenomenon: since the section of the diagonals is relatively small, their influence on the tensile rigidity and thus the bending stiffness can be neglected.
Looking at the comparison for the 3-dimensional construction, the differences for the 1st and 2nd case are also small. In the 3rd and 4th case, a similar behaviour is found as for the 2-dimensional construction: if the diagonals have a larger section than the verticals, their contribution in the bending stiffness becomes more apparent. However, the difference in percentages is larger for the 3-dimensional than for the 2-dimensional construction, 2.4% and 4.5% in the 3rd case, respectively. This prolific augmentation can be explained in view of the stress distribution in a tube construction compared to that in a trussed frame: in a tube construction, the tensile rigidity plays a relatively more important role due to the two "flanges" that are activated. Therefore the influence of the diagonals increases as well.

Summary: the approximation for the shear deflection of the geometry is nearly exact in all cases. However, the bending deflection varies when calculated by hand and computer. These differences are correlated with the influence of the diagonals on the bending stiffness which is neglected in the mechanics formulae.

TFC variant "diagonal columns"

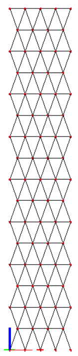

Figure 9.25: 2-dimensional variant

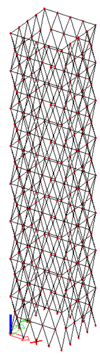

Figure 9.26: 3-dimensional variant

A (m^2)		δ	Hand (mm)	SCIA ESA PT (mm)	difference
A_h = 5.24e-2	O	$\delta_{bending}$	2141	2102	1.8%
A_d = 5.24e-2	O	δ_{shear}	152.3	153	-0.5%
		δ_{total}	2293	2255	1.7%
A_h = 1.29e-2	O	$\delta_{bending}$	8695	8539	1.8%
A_d = 1.29e-2	O	δ_{shear}	618.5	619.3	-0.1%
		δ_{total}	9314	9158	1.7%
A_h = 1.29e-2	O	$\delta_{bending}$	2604	2393	8.1%
A_d = 5.24e-2	O	δ_{shear}	152.3	153	-0.5%
		δ_{total}	2756	2546	7.6%
A_h = 5.24e-2	O	$\delta_{bending}$	8232	8211	0.3%
A_d = 1.29e-2	O	δ_{shear}	618.5	618.7	0.0%
		δ_{total}	8850	8830	0.2%

Table 9.4: Differences 2-dimensional geometry variant "diagonal columns".

A (m^2)		δ	Hand (mm)	SCIA ESA PT (mm)	difference
A_h = 5.24e-2	O	$\delta_{bending}$	510	516.3	-1.3%
A_d = 5.24e-2	O	δ_{shear}	152.3	152.5	-0.2%
		δ_{total}	662	668.8	-1.0%
A_h = 1.29e-2	O	$\delta_{bending}$	2070	2099	-1.4%
A_d = 1.29e-2	O	δ_{shear}	618.5	619.3	-0.1%
		δ_{total}	2689	2718	-1.1%
A_h = 1.29e-2	O	$\delta_{bending}$	620	569.9	8.1%
A_d = 5.24e-2	O	δ_{shear}	152.3	153	-0.5%
		δ_{total}	772	722.9	6.4%
A_h = 5.24e-2	O	$\delta_{bending}$	1960	2031	-3.6%
A_d = 1.29e-2	O	δ_{shear}	618.5	618.7	0.0%
		δ_{total}	2578	2650	-2.8%

Table 9.5: Differences 3-dimensional geometry variant "diagonal columns".

Regarding the 2-dimensional variant; in the 1st and 2nd case the differences are relatively small. Yet in the 3rd case the difference is substantial, which can be subscribed to the difference in bending deflection: the bending deflection calculated by ESA PT is smaller, meaning a larger bending stiffness. This effect can be explained by the fact that horizontal displacements at the base of the computer model are restricted. Indirectly, this is translated into an increased bending stiffness of the bottom part; the bottom part is the most important to limit the deflection at the top, hence the relatively large effect of 8.1%. This phenomenon is apparent in the 3rd case where the horizontals have a small section and the diagonals a large section. In the 4th case, where the sections are inversed, the differences are marginal: the horizontal displacements – and thus of the deforming of the rhomboids – are restricted by the relatively large sections of the horizontals.

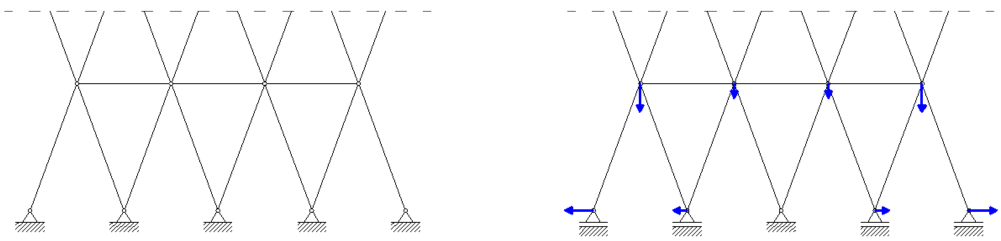

Figure 9.27: Restricted versus free movement at the base

Overall, the deflection calculated by computer is smaller for the 2-dimensional construction in all 4 cases due to a larger bending stiffness. The larger bending stiffness can be explained by the fact that the base of computer model has a larger width, whereas the hand calculation is based on the width between the lines of action, as illustrated in Figure 9.28 and Figure 9.29. If the model was infinitely tall, the results from the hand and the computer calculations would converge.

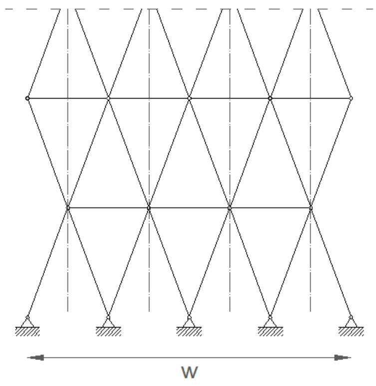

Figure 9.28: Effective width at the base of the computer model

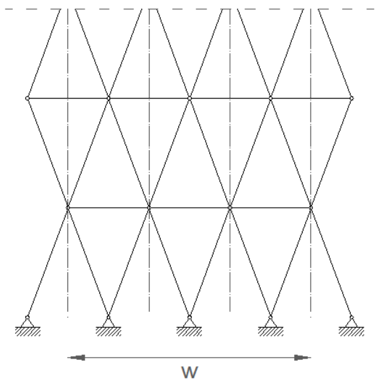

Figure 9.29: Effective width at the base of the hand calculations

Looking at the comparison for the 3-dimensional construction, the differences for the 1st and 2nd case are also small. Similarly, in the 3rd case the effect of the restricted movement for the computer model also results in a smaller deflection at the top. The effect of the greater width of the base and hence a greater bending stiffness is marginalized due to the floor plan with a square perimeter.

Additionally, the conclusion that can be drawn from the comparison is that the horizontal members every sixth storey – where the construction is at the smallest – do not actually contribute to the shear or bending stiffness: they have not been included in the hand calculation, though they are present in the ESA models. To verify their contribution, the secondary horizontal in the ESA models have been left out and the deflections have been computed again.

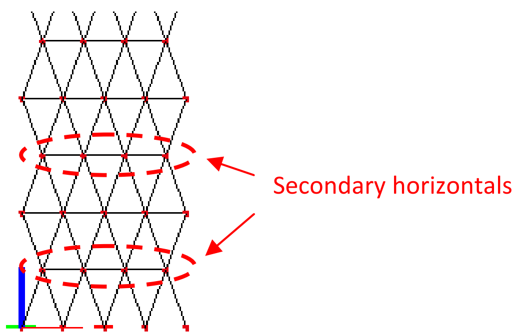

Figure 9.30: Omitted secondary horizontals in geometry variant "diagonal columns"

A (m^2)		δ	Hand (mm)	SCIA ESA PT (mm) (without sec. hor.)	difference	SCIA ESA PT (mm)
A_h = 5.24e-2	O	$\delta_{bending}$	2141	2107	1.6%	2102
A_d = 5.24e-2	O	δ_{shear}	152.3	152.5	-0.2%	153
		δ_{total}	2293	2260	1.5%	2255

A (m^2)		δ	Hand (mm)	SCIA ESA PT (mm) (without sec. hor.)	difference	SCIA ESA PT (mm)
A_h = 5.24e-2	O	$\delta_{bending}$	510	520.8	-2.2%	516.3
A_d = 5.24e-2	O	δ_{shear}	152.3	152.5	-0.2%	152.5
		δ_{total}	662	673.3	-1.7%	668.8

The computer results calculated with the new models without secondary horizontals are compared with the original hand calculations and the differences are shown. This has been done for the 2-dimensional and the 3-dimensional construction without any variation in the sections. The right column shows the initial results from the ESA models with the secondary horizontals still present. The comparison proves that the secondary horizontals do not contribute to the rigidity and can be left out.

Summary: the approximation for the shear deflection of the geometry is nearly exact in all cases. However, the bending deflection varies when calculated by hand and computer. These differences are correlated with the influence of the restricted movements and a different effective width at the base of the model on the bending stiffness. Furthermore, the comparison showed that the secondary horizontals can be omitted.

TFC variant "diagonal & vertical columns"

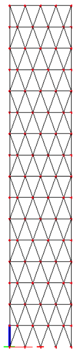

Figure 9.31: 2-dimensional variant

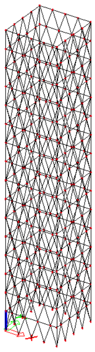

Figure 9.32: 3-dimensional variant

A (m^2)		δ	Hand (mm)	SCIA ESA PT (mm)	difference
A_h = 5.24e-2	O	$\delta_{bending}$	1054	1039	1.4%
A_d = 5.24e-2	O	δ_{shear}	152.3	153	-0.5%
A_v = 5.24e-2	O	δ_{total}	1206	1192	1.2%
A_h = 1.29e-2	o	$\delta_{bending}$	4282	4223	1.4%
A_d = 1.29e-2	o	δ_{shear}	618.5	619.3	-0.1%
A_v = 1.29e-2	o	δ_{total}	4901	4842	1.2%
A_h = 5.24e-2	O	$\delta_{bending}$	1707	1679	1.7%
A_d = 5.24e-2	O	δ_{shear}	152.3	152.5	-0.2%
A_v = 1.29e-2	o	δ_{total}	1860	1832	1.5%
A_h = 1.29e-2	o	$\delta_{bending}$	1156	1104	4.5%
A_d = 5.24e-2	O	δ_{shear}	152.3	153	-0.5%
A_v = 5.24e-2	O	δ_{total}	1308	1257	3.9%
A_h = 5.24e-2	O	$\delta_{bending}$	1659	1645	0.8%
A_d = 1.29e-2	o	δ_{shear}	618.5	618.7	0.0%
A_v = 5.24e-2	O	δ_{total}	2277	2264	0.6%
A_h = 5.24e-2	O	$\delta_{bending}$	4167	4142	0.6%
A_d = 1.29e-2	o	δ_{shear}	618.5	618.7	0.0%
A_v = 1.29e-2	o	δ_{total}	4785	4761	0.5%

A_h = 1.29e-2	o	$\delta_{bending}$	1990	1858	6.6%
A_d = 5.24e-2	O	δ_{shear}	152.3	153	-0.5%
A_v = 1.29e-2	o	δ_{total}	2142	2011	6.1%
A_h = 1.29e-2	o	$\delta_{bending}$	1677	1658	1.1%
A_d = 1.29e-2	o	δ_{shear}	618.5	619.3	-0.1%
A_v = 5.24e-2	O	δ_{total}	2295	2277	0.8%

Table 9.6: Differences 2-dimensional geometry variant "diagonal & vertical columns".

A (m^2)		δ	Hand (mm)	SCIA ESA PT (mm)	difference
A_h = 5.24e-2	O	$\delta_{bending}$	409	412.5	-0.8%
A_d = 5.24e-2	O	δ_{shear}	152.3	152.5	-0.2%
A_v = 5.24e-2	O	δ_{total}	562	565	-0.6%
A_h = 1.29e-2	o	$\delta_{bending}$	1662	1677	-0.9%
A_d = 1.29e-2	o	δ_{shear}	618.5	619.3	-0.1%
A_v = 1.29e-2	o	δ_{total}	2281	2296	-0.7%
A_h = 5.24e-2	O	$\delta_{bending}$	481	468.5	2.5%
A_d = 5.24e-2	O	δ_{shear}	152.3	152.5	-0.2%
A_v = 1.29e-2	o	δ_{total}	633	621	1.9%
A_h = 1.29e-2	o	$\delta_{bending}$	477	445.8	6.6%
A_d = 5.24e-2	O	δ_{shear}	152.3	153	-0.5%
A_v = 5.24e-2	O	δ_{total}	630	598.8	4.9%
A_h = 5.24e-2	O	$\delta_{bending}$	1008	1021	-1.2%
A_d = 1.29e-2	o	δ_{shear}	618.5	618.7	0.0%
A_v = 5.24e-2	O	δ_{total}	1627	1640	-0.8%
A_h = 5.24e-2	O	$\delta_{bending}$	1590	1633	-2.7%
A_d = 1.29e-2	o	δ_{shear}	618.5	618.7	0.0%
A_v = 1.29e-2	o	δ_{total}	2209	2252	-1.9%
A_h = 1.29e-2	o	$\delta_{bending}$	578	533.4	7.6%
A_d = 5.24e-2	O	δ_{shear}	152.3	153	-0.5%
A_v = 1.29e-2	o	δ_{total}	730	686.4	6.0%
A_h = 1.29e-2	o	$\delta_{bending}$	1037	1039	-0.2%
A_d = 1.29e-2	o	δ_{shear}	618.5	619.3	-0.1%
A_v = 5.24e-2	O	δ_{total}	1655	1658	-0.2%

Table 9.7: Differences 3-dimensional geometry variant "diagonal & vertical columns".

Regarding the 2-dimensional variant; in all cases the differences are marginal except for the 4th and 7th case. In both cases, the horizontals have small sections and the diagonals have large sections – while the vertical section is large and small respectively. The explanation can be found in the same effect as for the geometry variant “diagonal columns”, where the movements at the base of the computer model are restricted yielding a smaller deflection. However the difference is less significant for this geometry variant since the vertical columns – which are not affected by the restricted movement – also contribute in the bending stiffness.
Regarding the 3-dimensional variant; the differences are marginal except for the 4th and 7th case – just as for the 2-dimensional variant. The differences can be explained in the same way as for the 2-dimensional construction.

Additionally, the conclusion that can be drawn from the comparison is that the horizontal members every sixth storey – where the construction is at the smallest – do not actually contribute to the shear or bending stiffness: they have not been included in the hand calculation, though they are present in the ESA models. To verify their contribution, the secondary horizontal in the ESA models have been left out and the deflections have been computed again.

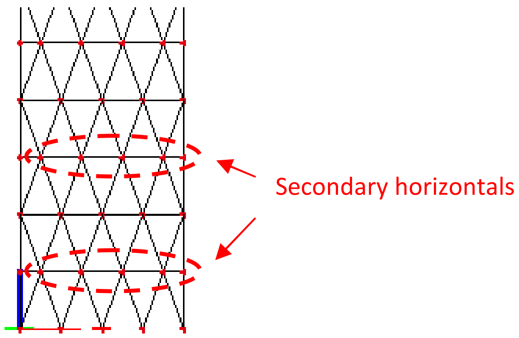

Figure 9.33: Omitted secondary horizontals in geometry variant “diagonal & vertical columns”

A (m^2)		δ	Hand (mm)	SCIA ESA PT (mm) (without sec. hor.)	difference	SCIA ESA PT (mm)
A_h = 5.24e-2	O	$\delta_{bending}$	1054	1040	1.3%	1039
A_d = 5.24e-2	O	δ_{shear}	152.3	152.5	-0.2%	153
A_v = 5.24e-2	O	δ_{total}	1206	1193	1.2%	1192

A (m^2)		δ	Hand (mm)	SCIA ESA PT (mm) (without sec. hor.)	difference	SCIA ESA PT (mm)
A_h = 5.24e-2	O	$\delta_{bending}$	409	415.3	-1.5%	412.5
A_d = 5.24e-2	O	δ_{shear}	152.3	152.5	-0.2%	152.5
A_v = 5.24e-2	O	δ_{total}	562	567.8	-1.1%	565

The computer results calculated with the new models without secondary horizontals are compared with the original hand calculations and the differences are shown. This has been done for the 2-dimensional and the 3-dimensional construction without any variation in the sections. The right column shows the initial results from the ESA models with the secondary horizontals still present. The comparison proves that the secondary horizontals do not contribute to the rigidity and can be left out.

Summary: the approximation for the shear deflection of the geometry is nearly exact in all cases. However, the bending deflection varies when calculated by hand and computer. These differences are correlated with the influence of the restricted movements and a different effective width at the base of the model on the bending stiffness. Furthermore, the comparison showed that the secondary horizontals can be omitted.

General conclusion

The hand calculations, based on the mechanics formulae, give a good approximation of the reality. The calculated shear deflection is an accurate approach while the bending deflection still shows some deviations. However, the order of these deviations is minor and, more important, can be estimated based on the comparison with the computer results for different sections. Therefore, the mechanics formulae seem reliable and a good base for the further design calculations.